ACCOUNTS of chemical research

Article

pubs.acs.org/accounts

Activating Nonreducible Oxides via Doping

Published as part of the Accounts of Chemical Research special issue "Microscopic Insights into Surface Catalyzed Chemical Reactions".

Niklas Nilius*,† and Hans-Joachim Freund‡

†Carl von Ossietzky University, Department of Physics, 26111 Oldenburg, Germany

‡Fritz-Haber-Institut der Max-Planck-Gesellschaft, 14195 Berlin, Germany

CONSPECTUS: Nonreducible oxides are characterized by large band gaps and are therefore unable to exchange electrons or to form bonds with surface species, explaining their chemical inertness. The insertion of aliovalent dopants alters this situation, as new electronic states become available in the gap that may be involved in charge-transfer processes. Consequently, the adsorption and reactivity pattern of doped oxides changes with respect to their nondoped counterparts. This Account describes scanning tunneling microscopy (STM) and photoelectron spectroscopy (XPS) experiments that demonstrate the impact of dopants on the physical and chemical properties of well-defined crystalline oxide films. For this purpose, MgO and CaO as archetypical rocksalt oxides have been loaded either with high-valence (Mo, Cr) or low-valence dopants (Li). While the former generate filled states in the oxide band gap and serve as electron donors, the latter produce valence-band holes and give rise to an acceptor response. The dopant-related electronic states and their polarization effect on the surrounding host material are explored with XPS and STM spectroscopy on nonlocal and local scales. Moreover, charge-compensating defects were found to develop in the oxide lattice, such as Ca and O vacancies in Mo- and Li-doped CaO films, respectively. These native defects are able to trap the excess charges of the impurities and therefore diminish the desired doping effect.

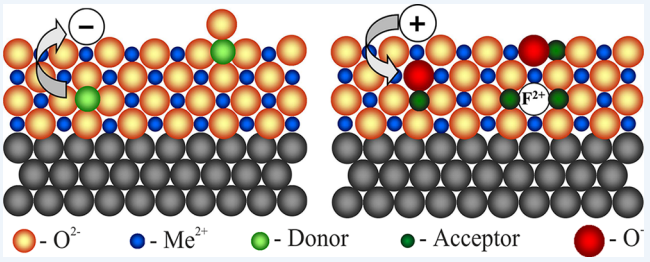

If noncompensated dopants reside in the host lattice, electron exchange with surface species is observed. Mo ions in CaO, for example, were found to donate electrons to surface Au atoms. The anionic Au strongly binds to the CaO surface and nucleates in the form of monolayer islands, in contrast to the 3D growth prevailing on pristine oxides. Charge transfer is also revealed for surface O_2 that traps one Mo electron by forming a superoxo-species. The activated oxygen is characterized by a reinforced binding to the surface, an elongated O−O bond length, and a reduced barrier for dissociation, and represents an important intermediate for oxidation reactions. The charge-transfer processes described here are quenched if Li is inserted into the oxide lattice, neutralizing the effect of the extra electrons. The specific behavior of doped oxides has been explored on a mechanistic level, i.e. on thin-film model systems at ultrahigh vacuum and low temperature. We believe, however, that our results are transferrable to realistic conditions and doping might thus develop into a powerful method to improve the performance of nonreducible oxides in surface-catalyzed reactions.

1. INTRODUCTION

Oxide materials play a fundamental role in surface-catalyzed chemical reactions. They fulfill two major purposes in heterogeneous catalysis. On the one hand, they serve as support material for the chemically active species, for example, an ensemble of metal particles. On the other, they may participate in the chemical reaction themselves, e.g., by providing charges for redox processes or balancing the oxygen supply. The two tasks are often fulfilled by different types of materials, nonreducible and reducible oxides. The first class contains main-group metals, such as Mg, Ca, Al, or Si. Their oxides are characterized by a fixed stoichiometry, a mainly ionic binding scheme, large band gaps, and high formation energies for defects. The nonreducible oxides are ideal support materials, because they are chemically inert and exhibit high temperature resistivity. In contrast, reducible oxides made of transition or rare-earth metals plus oxygen have an intrinsic redox potential, because the cationic species is able to change oxidation state. In order to keep the compound charge neutral, the process is balanced by the insertion of defects, typically O vacancies. Since reducibility is often accompanied by low defect formation energies, reducible oxides are ideal buffer materials for O_2 in chemical reactions. However, temperature and chemical inertness are lower than for their nonreducible counterparts.

In many applications, the favorable properties of reducible and nonreducible oxides shall be combined, for instance, to enable charge-transfer reactions between metal particles or adsorbates and the oxide support. A common approach in this regard is the insertion of defects into nonreducible oxides, for

Received: January 13, 2015
Published: April 20, 2015

DOI: 10.1021/acs.accounts.5b00018
Acc. Chem. Res. 2015, 48, 1532−1539

example, O-vacancies (or F-centers), which can be stabilized in different charge states and therefore add to the redox power of the material.[1] The main disadvantage of the method is the thermal fluxionality of defects, which tend to diffuse toward the surface, where they neutralize with their antipodal defect type. Especially at elevated reaction temperatures, the defect density continuously decreases, and the redox potential of the material vanishes over time. A more promising approach is the insertion of aliovalent dopants, which are firmly anchored in the lattice, for instance by their larger radius, and thus provide stable redox-centers even in nonreducible oxides.[2] Moreover, concentration, spatial distribution, and redox power of the charge centers can be adjusted independently of the oxide growth conditions, which is impossible for a defect ensemble. Finally, dopants residing directly in the surface may interact with adsorbates, further increasing the chemical versatility of the material.

In this Account, we review our experimental expertise to prepare doped oxides and discuss the impact of the impurities on structural and electronic properties of the host lattice. In addition, we analyze the role of the dopants in adsorption and growth processes at the surface. We take a fundamental viewpoint to discuss the physics and chemistry of doped oxides, as we use scanning tunneling microscopy (STM) and X-ray photoelectron spectroscopy (XPS) to characterize our samples. Both methods are capable of providing mechanistic insights into the role of dopants in the oxide lattice.

2. PREPARATION OF DOPED OXIDE FILMS

All experiments described here exploit the surface-science methodology and therefore require a finite conductivity of the sample. Because most nonreducible oxides are insulators even in the doped state, we have mimicked their properties by growing oxide films on metal single crystals. We have focused on the thickness range of 10−50 ML, thick enough to suppress the substrate influence at the oxide surface but sufficiently thin to avoid charging effects. In this regime, STM data can be acquired only at voltages outside the fundamental band gap, because electrons are transported via hopping through the oxide bands and not via tunneling.[3] Note that the necessary bias values are often too high to achieve atomic resolution on the oxide surface.

Two approaches were employed to prepare oxide films with a controlled doping level. In the first one, the host material was evaporated simultaneously with the dopants in an O_2 ambience of 10^{-5} to 10^{-7} mbar. The scheme was used for example to load MgO thin films with either Cr, Eu, or Li impurities.[4,5] The main drawback of the technique was the uncontrolled diffusion of the dopants during film annealing, followed by the formation of dopant-rich surface phases (Figure 1a,b). In contrast, segregation of substrate atoms into the oxide film was exploited in the second approach, used for instance to prepare Mo-doped CaO (Figures 1c,d.). Upon CaO deposition on the Mo(001) support, a considerable misfit strain is generated at the interface due to the 8% larger lattice parameter of the oxide. The strain gets partly released by incorporating up to 25% Mo ions into the growing film, because the Mo−O bond length is considerably shorter than the Ca−O distance.[6] The mixed oxide at the interface now forms an ideal starting point for Mo diffusion into the CaO matrix, whereby the desired Mo concentration in a near-surface region can be adjusted by changing either the film thickness or the growth temperature.[7] Although strain-driven diffusion avoids dopant accumulation at the surface, it generates a falling doping profile when moving away from the metal support. Other doping techniques involve high-energy sputtering of impurities as well as various wet-chemical approaches but will not be discussed in this Account.

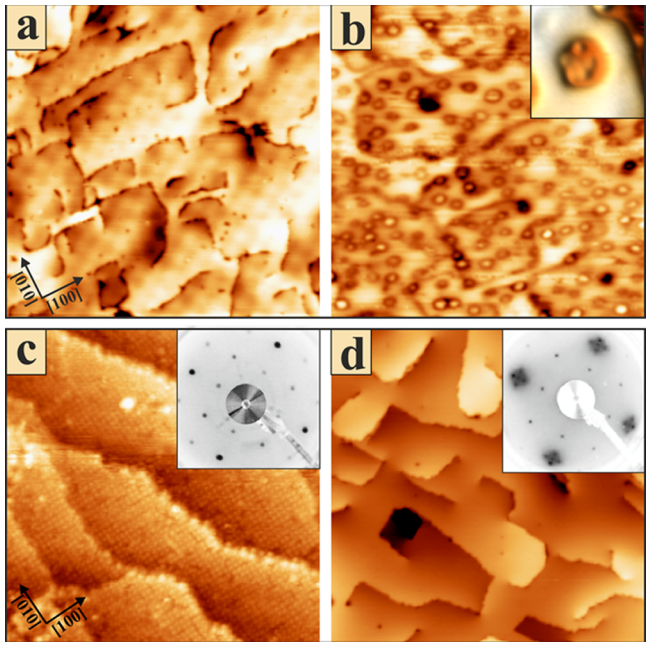

Figure 1. (a) STM image of a pristine 10 ML thick MgO film grown on Mo(001) and (b) MgO_{Eu} prepared by Mg and Eu coevaporation in O_2 and annealing to 1000 K (140 × 140 nm^2). At this temperature, Eu segregates to the surface and forms small Eu_2O_3 islands (inset). (c) STM image of 3 ML (25 × 25 nm^2) and (d) 25 ML CaO grown on Mo(001) (80 × 80 nm^2). While the (2 × 2) LEED superstructure in panel c is indicative of a mixed Ca−Mo oxide, the (1 × 1) pattern in panel d is compatible with the (doped) bulk CaO lattice.

3. ELECTRONIC AND MORPHOLOGICAL PROPERTIES OF DOPED OXIDES

In order to verify the existence of dopants in the oxide lattice and to probe their electronic impact, we have investigated the state-density of doped oxide films via XPS and STM conductance spectroscopy (STS). The results are discussed mainly for CaO_{Mo}, a rocksalt lattice with Mo impurities populating a few Ca substitutional sites. Upon annealing from 700 to 1100 K, XPS measurements revealed a pronounced shift of the Ca 2p and O 1s core levels to higher binding energy (Figure 2a). The shift reflects the interdiffusion of Mo ions into the oxide at rising temperature, where they replace some of the divalent Ca species.[8] Because the +2 charge of rocksalt cations is energetically unfavorable for Mo, especially the near-interface dopants switch spontaneously into a higher oxidation state by donating electrons back to the metal support.[9] This interfacial charge transfer generates a positive dipole between the electron-donating film and the underlying substrate, causing the oxide electronic states to shift to higher binding energy. The effect is restricted to a near-interface region and vanishes with increasing film thickness due to the limited transfer length of electrons in the insulating oxide. Near surface dopants therefore maintain their donor capacity, enabling them to alter the adsorption behavior of the film as discussed in section 4.

Similar results were obtained from local STS measurements, addressing the behavior of CaO states near the Fermi level. Also here, an upshift of the CaO conduction band was revealed

DOI: 10.1021/acs.accounts.5b00018
Acc. Chem. Res. 2015, 48, 1532−1539

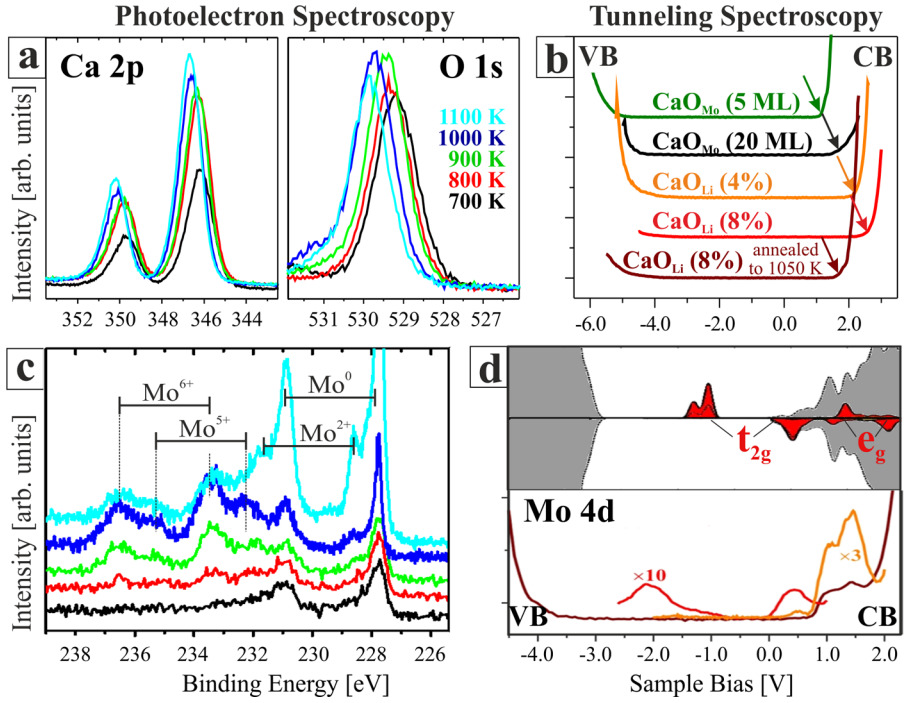

Figure 2. (a, c) XP spectra of the Ca 2p and O 1s core levels and the Mo 3d impurity states measured as a function of the annealing temperature of CaO_{Mo} (600 eV photon energy). (b) STM spectra of the CaO band gap, illustrating the band-shift effects due to charged dopants in the film. (d) High resolution STS curve of CaO_{Mo} with the Mo 4d states appearing in the band gap. Their position can be qualitatively compared with DFT calculations presented above.[12]

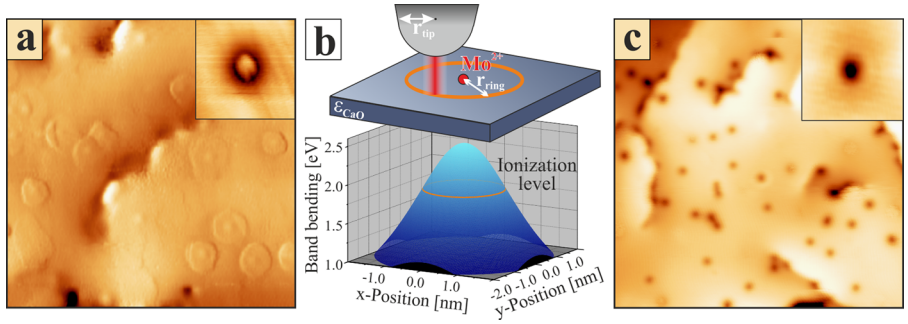

Figure 3. (a) STM image of 25 ML CaO, showing characteristic Mo-induced charging rings (30 × 30 nm^2). (b) Real-space model of a charging ring and underlying shift of the Mo^{2+} HOMO calculated for 5.0 V sample bias and 2.5 nm tip radius. Electron transfer into the CaO conduction band takes place if the level crosses the orange line. (c) STM image of CaO_{Mo} annealed to 1000 K, exhibiting a high density of V_{Ca} defects (30 × 30 nm^2). Individual defects are depicted in the insets (5 × 5 nm^2).

with increasing film thickness, reflecting the vanishing influence of the charge-transfer dipole at the interface (Figure 2b).[8] Whereas the band onset was determined to 1.5 V in 5 ML thick films, it moved to 2.0 V at 20 ML thickness. Experiments on Li-doped CaO confirmed that the band shift indeed originates from the electronic response of the dopants.[10] Li, as a monovalent species, serves as electron acceptor in the CaO lattice and produces hole states in the O 2p derived valence band.[11] Due to their high energy, the holes in interfacial oxide layers get immediately filled with electrons from the support. The electron transfer between oxide and Mo(001) therefore changes direction, and the conduction band moves to higher energy with increasing Li concentration, reflecting the destabilizing role of the extra electrons (Figure 2b).

However, not only the dielectric response of the host bands but also the occurrence of new electronic states induced by the impurities indicates the doped nature of the oxide. XPS is most sensitive to the Mo 3d states that produce various sharp doublets at 228–237 eV binding energy.[8] From their energy position and intensity, information on charge state and concentration of the dopant ions can be derived. While in as-grown, hence dopant-free, CaO films, only a weak remnant of the Mo^0 states of the support is detected, a new doublet at 229 eV, typical for Mo^{2+} and Mo^{3+}, suggests the diffusion of Mo ions into the film upon annealing (Figure 2c). With increasing temperature, the bands intensify as more Mo enters the lattice. Above 1000 K, the oxide film decomposes and a highly oxidized Mo species emerges in the spectra, as indicated by new XPS lines above 232 eV. Further evidence for single-ion Mo impurities in the CaO lattice comes from the STS data shown in Figure 2d.[12] Whereas the rising conductance signal on the left and right side of the curve marks the onset of the CaO valence and conduction band, respectively, states inside the gap relate to the 4d levels of the Mo dopants. As shown by

DOI: 10.1021/acs.accounts.5b00018
Acc. Chem. Res. 2015, 48, 1532–1539

associated DFT calculations,[12] the 4d states split in the CaO crystal field into a low-lying t_{2g} and a high-lying e_g manifold. Whereas the e_g states are entirely empty, the t_{2g} levels contain four Mo 4d electrons in the Mo^{2+} species, forming the basis for the donor character of the material. We note that the dopant electronic structure has been analyzed also by STM luminescence spectroscopy, using the emission response of the oxide after electron injection from the tip.[5] For example, Cr-doped MgO features a sharp 700 nm emission peak due to $e_g \rightarrow t_{2g}$ transitions inside the gap,[4] while Li-doped MgO emits 550 nm light arising from the recombination of electrons in Li-induced F^{2+} centers and holes in the oxide valence band.[13]

The distinct electronic structure of transition metal ions in rocksalt oxides gives rise to an unusual charging mechanism that renders individual dopants visible in the STM, although no atomic resolution is obtained on the insulator and most dopants reside below the surface.[14] Especially on well-ordered CaO_{Mo} films, concentric rings with diameters depending on imaging bias and film thickness can be detected (Figure 3a). The rings reflect a temporary charging of the Mo impurities in the oxide lattice, triggered by the electric field of the STM tip (Figure 3b).[15] At negative tip bias used for imaging, the oxide bands experience a localized upward bending around the tip position. The Mo-induced gap states follow this trend, whereby the highest occupied orbitals may shift above the conduction band onset in a more distant, hence less affected, CaO region. At this condition, Mo transfers one electron to the CaO matrix and becomes oxidized. The resulting positive net-charge polarizes the surrounding oxide and changes its imaging contrast in the STM, producing the concentric rings seen in Figure 3a. Using calculated energy gaps between the highest occupied Mo 4d states and the conduction band onset, the ring diameter has been correlated with the charge state and position of the Mo donor.[14] The analysis revealed that only Mo^{2+} ions in the first three subsurface layers are susceptible to a tip-induced ionization and give rise to the charging rings seen on the surface. For higher Mo oxidation states or positions deeper inside the film, either the energy gap is too large or the tip electric field is too weak to stimulate charge-transfer processes out of the impurities. Because tip-induced switches of the oxidation state require similar electronic preconditions as a permanent charge transfer into an adsorbate, the ring-producing entities will be particularly relevant for the donor character of the doped oxide. However, not all impurities remain in the required low oxidation state as electron-trapping lattice defects easily develop in the doped oxides, as discussed next.

The most abundant defect on the CaO_{Mo} surface, besides the charging rings, shows up as a circular depression of 1.0 nm diameter (Figure 3c). It was identified as a Ca vacancy located in the topmost oxide plane.[16] In stoichiometric films, this defect has prohibitively large formation energy, for example, 8 eV for a V_{Ca} in CaO, and O vacancies consequently govern the defect landscape of main-group oxides. The development of cationic defects is however the typical response to the presence of high-valence dopants in the compound. In fact, stabilization of a Mo donor in the +2 oxidation state is unfavorable in CaO, because it involves energy-costive population of the 4d levels high in the band gap. While further oxidation of the Mo is hindered by the absence of suitable acceptor states in the ideal lattice, such traps can be produced by removing an oxide cation that leaves behind two holes in adjacent oxygen ions. These hole states readily accept the extra charges from a nearby donor, which consequently switches into a higher oxidation state. Cationic vacancies thus serve as compensating defects for high-valence ions in the rocksalt lattice, which explains the drastic reduction of their formation energy ($E_{V_{Ca}}$ = 1.5 eV)[17] and their abundance in the CaO film, as shown in Figure 3c. For MgO_{Cr}, the charge redistribution via native defects is so efficient that all Cr ions are stabilized in the favorable +3 charge state and the donor character of the doped oxide vanishes.[17] We emphasize that not only point but also line defects are potentially able to trap electrons from donor-type impurities.[18]

In contrast to high-valence dopants, low-valence impurities tend to stabilize oxygen vacancies (F centers) as the archetypical electron-releasing defect. While mainly charge neutral F^0 centers are observed in pristine oxides, positive F^{2+} centers occur in oxides doped with low-valence impurities.[19] The two electrons that were originally trapped in the F^0 centers are hereby transferred to the low-coordinated O ions produced by the dopants, a process that drastically reduces the formation energy of the respective O vacancy. Moreover, the desired acceptor character of the doped oxide is largely suppressed by the compensating defects, which rationalizes, for example, the low chemical activity of Li-doped MgO.[19]

Formation of charge-compensating defects needs to be considered whenever the redox potential of a nonreducible oxide shall be altered via doping. Charge centers may only be generated in the lattice if the formation of compensating vacancies is energetically unfavorable compared to stabilizing the dopants in a low oxidation state.[20] A successful insertion of electron-rich donors, on the other hand, has dramatic consequences on the adsorption and reaction behavior of doped oxides.

4. ADSORPTION PROPERTIES OF DOPED OXIDES

The oxidation state of an adsorbate often governs its binding potential, as excess charges enable new interaction mechanisms to an ionic material. Typical charge-mediated binding schemes are Coulomb attraction between opposite charges or polaronic lattice distortions, in which the surface ions get displaced in order to accommodate the charged adsorbate. The efficiency of polaronic binding was proven by DFT calculations that revealed a two times stronger adsorption of a Au^- species to MgO(001) than of its neutral counterpart (1.5 versus 0.8 eV).[21] The effect vanishes for rigid lattice geometries that are unable to respond to the extra charges.[22] Charge-mediated binding schemes are therefore expected to govern the adsorption behavior of doped oxides.

The phenomenon was first realized for CaO_{Mo} films exposed to a submonolayer of gold.[12] As most other metals, Au forms 3D crystallites when dosed onto pristine CaO, given the negligible adhesion to the wide-gap material.[23] Doping with high-valence Mo ions changes the binding behavior, and the incoming Au atoms now aggregate into monolayer islands with hexagonal symmetry, indicative of the (111) character of the underlying Au lattice (Figure 4a,b). The reduced island height provides evidence for a reinforced metal-oxide adhesion, reflecting the effect of the dopants. DFT calculations disclosed that near-surface Mo ions are efficient donors to the incoming Au atoms, because their highest occupied 4d level lies above the lowest unoccupied Au state.[12] Consequently, an electron from the Mo HOMO spontaneously moves to the Au 6s affinity level and triggers the formation of a Au^- species. Its binding energy to the CaO surface increases by almost a factor of 3 after the

DOI: 10.1021/acs.accounts.5b00018
Acc. Chem. Res. 2015, 48, 1532−1539

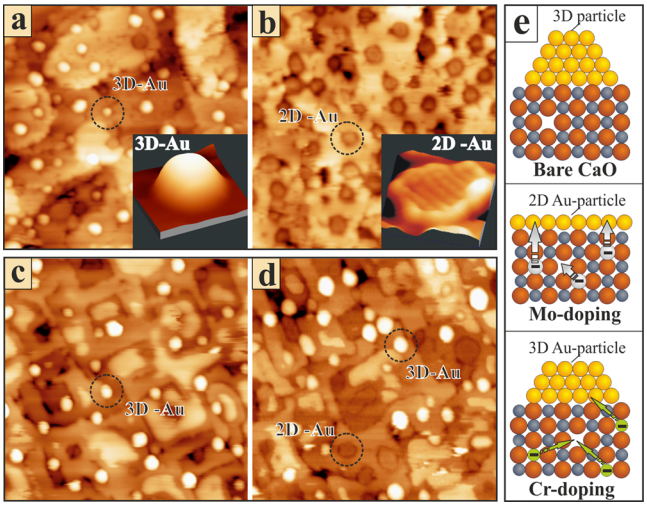

Figure 4. STM images of (a) pristine and (b) Mo-doped CaO films after dosing 0.5 ML of Au (60 nm × 50 nm). The insets show typical Au deposits on the nondoped and doped surface. (c, d) Similar data taken on bare and Cr-doped MgO(001). Note that 2D islands appear as faint depressions on both oxides, because electron transport through the gold is inhibited by the extra charges. (e) Charge transfer processes that govern the different growth modes of gold on bare/doped oxides.

charge transfer. Moreover, the enhancement is almost independent of the binding position (top or hollow, Ca or O site), demonstrating the efficiency of the polaronic lattice distortion induced by the charged adsorbate. Closer inspection of the different binding contributions indicates that not the formation of the Au^- species but the enhanced interaction of the oxidized donor to its O ligands causes most of the energy rise.[24] The increased metal-oxide adhesion now explains the observed 2D growth of gold, because this regime maximizes the number of Au atoms in contact with the oxide surface (Figure 4e). The transferred charges thereby take an uneven distribution inside the Au islands, with most electrons residing in the perimeter atoms.[25] By this means, the Coulomb repulsion between the excess electrons is minimized and further growth of the metal sheets gets promoted. The presence of an electron-rich perimeter should also be beneficial for redox processes taking place at the metal-oxide boundary.[26]

Further calculations revealed that Mo is a particularly effective donor, because it is able to transfer more than one electron to a Au island on the CaO surface.[17] In fact, not only the highest occupied t_{2g} orbital of a Mo^{2+} ion lies above the Au 6s affinity level, but also the HOMOs of Mo^{3+} and Mo^{4+} ions are susceptible to charge transfer. However, the energy gain becomes smaller with each transfer step, as the residual electrons get progressively stabilized by the Mo donor, which in turn limits the maximum distance for electron exchange. Nonetheless, CaO_{Mo} exhibits a robust donor characteristic, explaining why charge-related binding schemes are observable despite the unavoidable presence of native electron traps in the oxide lattice.[18]

The properties of Cr dopants are distinctively different, although Cr has a similar electronic structure as Mo but is a 3d instead of a 4d transition metal. Gold deposition onto Cr-doped MgO films results in the formation of 3D particles, and almost no evidence for charge-mediated binding is detected (Figure 4c,d). This is surprising at first glance, because Cr ions induce occupied crystal-field states into the MgO band gap as well.[17] However, these states are separated by wider gaps due to the larger MgO Madelung potential with respect to CaO and the higher multiple-ionization energies of the Cr species. As a result, only the $Cr^{2+} \rightarrow Cr^{3+}$ charging step can be triggered by the surface Au atoms, while higher oxidation states are inaccessible for Au as reducing agent. Moreover, the first Cr electron is often spontaneously released to the MgO before the gold has even been dosed to the surface. The reason is the rather low formation energy of Mg vacancies in the rocksalt lattice, rendering the formation of compensating defects feasible even at moderate temperature. Finally, the MgO film contains a high density of misfit dislocations that serve as intrinsic electron traps and promote spontaneous $Cr^{2+} \rightarrow Cr^{3+}$ oxidation.[27] The ideal donor-type impurity should thus be characterized by several high-lying electronic states, suitable for transferring more than one electron, while the host oxide should have a low Madelung potential and a small number of parasitic lattice defects. Beside Mo, other transition metals have

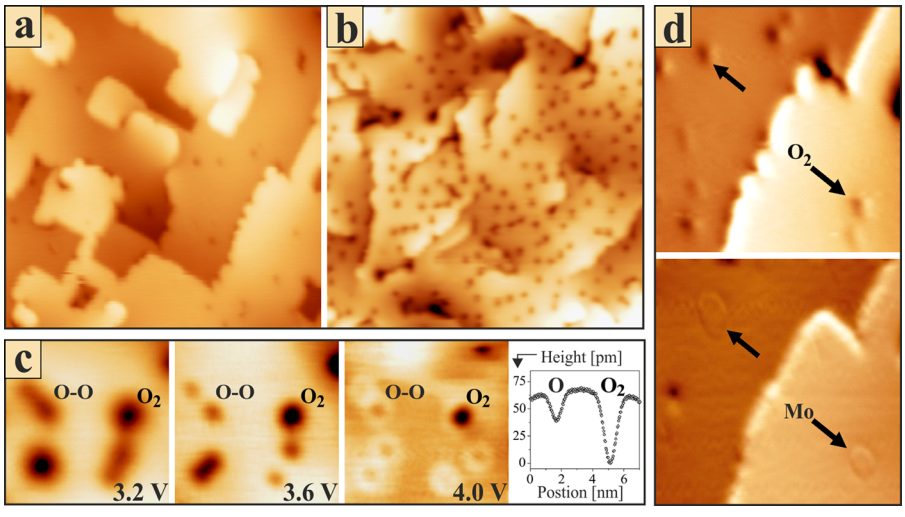

Figure 5. (a, b) STM images of bare and Mo-doped CaO after dosing 5 Langmuir O_2 at 20 K (40 × 40 nm^2). (c) Bias-dependent contrast and height profile of oxygen molecules (deep minima) and atoms (faint double dents). Note the dissociation of an O_2 in the lower left image part during scanning. (d) Appearance of Mo charging rings after desorbing two O_2 molecules from the surface (17 × 17 nm^2).

DOI: 10.1021/acs.accounts.5b00018
Acc. Chem. Res. 2015, 48, 1532−1539

been proposed by theory to develop reliable donor properties in CaO, for example, Nb and Ti;[28] an experimental verification is however missing at this point.

Not only native oxide defects but also low-valence dopants produce electron traps that potentially destroy the donor character of a doped oxide. To demonstrate this effect experimentally, we have prepared CaO_{Mo} films with an increasing amount of Li dopants and probed the charge-transfer capacity of the material by growing Au particles on top. As expected, monolayer Au islands, as an indication for the development of Au^- species, were observed only for low Li concentrations.[10] At higher doping level, more and more deposits followed a 3D growth regime, until all monolayer islands vanished at ∼8% Li amount. This result corroborates our charge-transfer concept. Monovalent Li acts as electron acceptor in the rocksalt lattice, because it cannot satisfy the coordinative needs of the O ions. The resulting holes in the O 2p states are readily filled with Mo excess electrons, which are consequently missing for charge exchange with the ad-gold. The donor potential of the material therefore diminishes and more Au atoms agglomerate into 3D particles, being typical for nondoped oxides. High-valence Mo and low-valence Li ions are therefore opponents in the charge-transfer response of a doped oxide.

The second example for a dopant-mediated adsorption scheme concerns oxygen. In analogy to gold, O_2 is a strong Lewis acid and able to trap electrons by forming super- or peroxo-species (O_2^- and O_2^{2-}). The associated charge transfer often represents a crucial step in oxidation reactions, as the extra electrons populate antibonding orbitals of the O_2 molecule and promote its dissociation. Most wide-gap insulators are chemically inert against oxygen, and molecular activation typically requires the presence of metal particles on the oxide surface.[29] This situation changes in the presence of high-valence dopants, as revealed from our O_2 adsorption experiments on CaO_{Mo}.[30] While the pristine oxide is unable to bind oxygen, a number of circular minima occur on the surface of doped CaO upon O_2 exposure (Figure 5a,b). We assign these new entities to molecular oxygen, because they can be dissociated via electron injection from the STM tip (Figure 5c). The manipulation results in two faint minima, depicting the atomic constituents of the molecule. Apparently, the high-valence dopants help stabilizing a molecular oxygen species with a high propensity for dissociation on the CaO surface.

The anticipated role of the dopants is verified by additional manipulation experiments, in which individual molecules are desorbed from the surface with 3.5 V tip pulses.[30] In most cases, a wide concentric ring emerges at the former O_2 binding site, the unambiguous signature for a Mo donor in a subsurface CaO plane (Figure 5d). From the fact that no charging ring is observed as long as the molecule resides on the surface, we conclude that the high-lying electrons have already left the Mo donor and were possibly transferred to the oxygen orbitals. This scenario is supported by an additional experiment that probes the local charge distribution on the CaO surface via the position of distinct vacuum states.[31] For this purpose, electron transport through the STM junction is measured at bias voltages above the sample work function, whereby the vacuum states appear as conductance maxima. Their energy position is governed by the tip electric field but more importantly by the presence of surface charges. While an electron surplus shifts the vacuum states to higher energy, positive charges cause a downshift. The level energy thus contains useful information on the type and concentration of surface charges. The vacuum states on CaO_{Mo} films experience a pronounced upshift by 0.5 eV upon O_2 exposure, indicating electron transfer toward the surface. The shift is completely reversible, and the states return to their original position after O_2 desorption. Apparently, the molecules exchange electrons with Mo donors in the CaO lattice, a process that has indeed been verified by DFT calculations.[30]

While pristine CaO interacts only weakly with O_2 (E_B = 0.13 eV on Ca−Ca bridge sites), the adsorption strength increases substantially on the doped oxide due to the formation of a superoxo O_2^- species. The new binding energy calculates to 0.87 eV for a Mo^{3+} ion in the third subsurface layer and increases further if a Mo^{2+} species acts as electron donor. The superoxo character of the adsorbate is proven by several indicators, an elongated O−O bond length, a reduced stretching frequency, and a higher spin state as compared to neutral oxygen. Moreover, the calculated O_2 dissociation barrier decreases from 1.14 to 0.68 eV upon charge transfer, reflecting the bond weakening after populating the antibonding π^* orbitals of the molecule.[30] The latter is in line with the facile O_2 dissociation with the STM tip. Charge transfer from Mo donors therefore strengthens the O_2 adsorption but concomitantly activates the molecule on the wide-gap oxide support.

In a final example, the efficiency of charge-transfer is addressed when more than one electron-accepting species is dosed onto a doped oxide. For this purpose, Au atoms and O_2 molecules were coadsorbed on the CaO_{Mo} films, and the resulting charge distribution was derived again from the 2D/3D growth behavior of gold. While both adsorbates are Lewis acids, Au atoms have a much higher electron affinity (2.3 eV) than O_2 molecules (0.5 eV). Indeed, the dominant Au particle shape was found to depend on the oxygen pressure during gold deposition.[32] Below 10^{-8} mbar O_2, gold nucleates exclusively in the form of monolayer islands, providing a clear hint for a charge-mediated binding scheme.[12] At higher oxygen dosage, an increasing number of Au deposits develop compact 3D shapes. Apparently, the surface O_2 drains more and more electrons from the Mo impurities, and the residual charges are not sufficient to induce a 2D growth for all aggregates. Interestingly, the growth behavior is perfectly bimodal in this stage and the gold forms either perfect 2D or 3D deposits. Above 10^{-6} mbar O_2, no monolayer islands are detected anymore, suggesting that most Au atoms remain neutral and follow the 3D growth behavior found on nondoped oxides. At these pressure conditions, every Au atom statistically competes with 100 O_2 molecules for excess charges, explaining why O_2 is more successful in trapping the Mo electrons despite its lower electron affinity. The experiments illustrate that the efficiency of charge transfer depends not only on intrinsic properties of the doped oxide but also on competing influences imposed by the surrounding gas phase.

5. CONCLUSIONS

This Account aimed at exploring the nature of doped oxides and at correlating charge-transfer processes with the distinct adsorption behavior of the material. We have discussed how dopants change the electronic structure of the host lattice, for example, by altering the energy of intrinsic oxide bands and inducing new states in the gap region. The interplay between aliovalent dopants and charge-compensating defects was discussed for cationic as well as oxygen vacancies. In fact, an abundance of compensating defects was found to annihilate the

DOI: 10.1021/acs.accounts.5b00018
Acc. Chem. Res. 2015, 48, 1532−1539

impact of the dopants, explaining why doped oxides do not always respond in the expected manner. Charge-transfer processes into suitable adsorbates were revealed in the presence of active dopants in the host lattice. Gold deposition onto electron-rich CaO_{Mo}, for example, resulted in the development of monolayer Au islands, in contrast to the 3D growth prevailing on nondoped oxides. Oxygen adsorption on CaO_{Mo} stimulated the formation of superoxo-species, characterized by an elongated O−O bond length and a reduced dissociation barrier. Dopant-induced O_2 activation might therefore present a decisive step for catalyzing oxidation reactions on oxide surfaces. The preparation of acceptor-type materials via low-valence dopants, as in MgO_{Li}, turned out to be difficult due to the low formation energy of the corresponding charge-compensating O defects.

The experiments described here gave insight into mechanistic properties of doped oxides, such as band bending and charge-transfer processes. Further studies are required to prove that the promoting effects of aliovalent dopants survive the harsh conditions of a real chemical reaction. Relevant points in this respect are the diffusion of dopants toward the surface and their segregation into new, inactive phases. Moreover, excess charges may leave the single-ion impurities and become trapped in lattice defects with high stability. Such unfavorable scenarios need to be invalidated with applied studies in the future in order to establish the beneficial impact of dopants in surface-catalyzed chemical reactions.

AUTHOR INFORMATION

Notes

The authors declare no competing financial interest.

Biographies

Niklas Nilius studied physics and received his Ph.D. in the group of H.-J. Freund for an investigation of the optical properties of single metal particles by STM luminescence spectroscopy. In 2002-2003, he worked as a postdoctoral fellow with Wilson Ho on the assembly of monatomic chains via STM manipulation techniques. In 2013, he became professor at Oldenburg University. His research is focused on the preparation and atomic-scale characterization of oxide materials for applications in chemistry and photovoltaics.

Hans-Joachim Freund studied physics and chemistry at the University of Cologne, where he received his Ph.D. in 1978 and his habilitation in 1983. He worked as a postdoctoral fellow in the Physics Department at the University of Pennsylvania before he became associate professor in Erlangen (1983) and full professor in Bochum (1987). Since 1995, he has been the director of the Chemical Physics Department at the Fritz-Haber-Institute of the Max-Planck-Society. He received several national and international awards, is a member of various academies, scientific societies, and journal advisory boards and serves as Honorary Professor at five universities.

ACKNOWLEDGMENTS

This Account would have been impossible without the fruitful collaboration with several theoreticians, in particular with Gianfranco Pacchioni, Livia Giordano, Joachim Sauer, and Hannu Häkkinen. The experimental results combine the work of many postdoctoral researchers in our group: Yi Cui, Yi Pan, Xiang Shao, and Fernando Stavale. The authors deeply acknowledge their hard and enthusiastic work in the past years.

REFERENCES

(1) Yoon, B.; Hakkinen, H.; Landman, U.; Worz, A. S.; Antonietti, J. M.; Abbet, S.; Judai, K.; Heiz, U. Charging Effects on Bonding and Catalyzed Oxidation of CO on Au_8 Clusters on MgO. *Science* **2005**, *307*, 403−407.
(2) McFarland, E. W.; Metiu, H. Catalysis by Doped Oxides. *Chem. Rev.* **2013**, *113*, 4391−4427.
(3) Cui, Y.; Tosoni, S.; Schneider, W.-D.; Pacchioni, G.; Nilius, N.; Freund, H.-J. Phonon-Mediated Electron Transport through CaO Thin Films. *Phys. Rev. Lett.* **2015**, *114*, No. 016804.
(4) Stavale, F.; Nilius, N.; Freund, H.-J. Cathodoluminescence of Near-Surface Centres in Cr-Doped MgO(001) Thin Films Probed by STM. *New J. Phys.* **2012**, *14*, No. 033006.
(5) Stavale, F.; Pascua, L.; Nilius, N.; Freund, H.-J. From Embedded Nanoislands to Thin Films: Topographic and Optical Properties of Europium-oxide on MgO(001) Films. *Phys. Rev. B* **2012**, *86*, No. 085448.
(6) Shao, X.; Nilius, N.; Myrach, P.; Freund, H.-J.; Martinez, U.; Prada, S.; Giordano, L.; Pacchioni, G. Strain-Induced Formation of Ultrathin Mixed-Oxide Films. *Phys. Rev. B* **2011**, *83*, No. 245407.
(7) Shao, X.; Myrach, P.; Nilius, N.; Freund, H.-J. Growth and Morphology of Calcium-Oxide Films Grown on Mo(001). *J. Phys. Chem. C* **2011**, *115*, 8784−8789.
(8) Cui, Y.; Pan, Y.; Pascua, L.; Qiu, H.; Stiehler, C.; Kuhlenbeck, H.; Nilius, N.; Freund, H.-J. Evolution of CaO Electronic Structure Following Mo Inter-diffusion at High Temperature. *Phys. Rev. B* **2015**, *91*, No. 035418.
(9) Prada, S.; Giordano, L.; Pacchioni, G. Substitutional Doping in MgO Films on Metals. *J. Phys. Chem. C* **2012**, *116*, 5781−5786.
(10) Shao, X.; Nilius, N.; Freund, H.-J. Li/Mo Codoping of CaO Films. *J. Am. Chem. Soc.* **2012**, *134*, 2532−2534.
(11) Sun, X. Y.; Li, Bo.; Metiu, H. Methane Dissociation on Doped CaO(001). *J. Phys. Chem. C* **2013**, *117*, 7114−7122.
(12) Shao, X.; Prada, S.; Giordano, L.; Pacchioni, G.; Nilius, N.; Freund, H.-J. Tailoring the Shape of Metal Ad-particles by Doping the Oxide Support. *Angew. Chem., Int. Ed.* **2011**, *50*, 11525−11527.
(13) Richter, N. A.; Stavale, F.; Levchenko, S. V.; Nilius, N.; Freund, H. J.; Scheffler, M. Li-Mediated Oxygen Vacancies in Bulk MgO. *Phys. Rev. B* **2015**, in press.
(14) Cui, Y.; Nilius, N.; Freund, H.-J.; Prada, S.; Giordano, L.; Pacchioni, G. Controlling the Charge State of Single Mo-Dopants in a CaO Film. *Phys. Rev. B* **2013**, *88*, No. 205421.
(15) Zheng, H.; Weismann, A.; Berndt, R. Manipulation of Subsurface Donors in ZnO. *Phys. Rev. Lett.* **2013**, *110*, No. 226101.
(16) Cui, Y.; Shao, X.; Prada, S.; Giordano, L.; Pacchioni, G.; Freund, H.-J.; Nilius, N. Surface Defects and Their Impact on the Electronic Structure of Mo-Doped CaO Films. *Phys. Chem. Chem. Phys.* **2014**, *16*, 12764−12772.
(17) Stavale, F.; Shao, X.; Nilius, N.; Freund, H.-J.; Prada, S.; Giordano, L.; Pacchioni, G. Donor Characteristics of Transition-Metal-Doped Oxides. *J. Am. Chem. Soc.* **2012**, *134*, 11380−11383.
(18) McKenna, K. P.; Shluger, A. Electron-Trapping Polycrystalline Materials with Negative Electron Affinity. *Nat. Mater.* **2008**, *7*, 859−862.
(19) Myrach, P.; Nilius, N.; Levchenko, S. V.; Gonchar, A.; Risse, T.; Dinse, K.-P.; Boatner, L. A.; Frandsen, W.; Horn, R.; Freund, H.-J.; Schlögl, R.; Scheffler, M. Temperature-Dependent Morphology, Magnetic, and Optical Properties of Li-doped MgO. *ChemCatChem* **2010**, *2*, 854−862.
(20) Robertson, J.; Clark, S. J. Limits to Doping in Oxides. *Phys. Rev. B* **2011**, *83*, No. 075205.
(21) Pacchioni, G.; Giordano, L.; Baistrocchi, M. Charging of Metal Atoms on Ultrathin MgO/Mo(100) Films. *Phys. Rev. Lett.* **2005**, *94*, No. 226104.
(22) Martinez, U.; Jerratsch, J.-F.; Nilius, N.; Giordano, L.; Pacchioni, G.; Freund, H.-J. Tailoring the Interaction Strength between Gold Particles and Silica Films via Work Function Control. *Phys. Rev. Lett.* **2009**, *103*, No. 056801.

DOI: 10.1021/acs.accounts.5b00018
Acc. Chem. Res. 2015, 48, 1532−1539

(23) Shao, X.; Nilius, N.; Freund, H.-J. Crossover from Two- to Three-Dimensional Gold Particle Shapes on CaO Films of Different Thicknesses. *Phys. Rev. B* **2012**, *85*, No. 115444.
(24) Andersin, J.; Nevalaita, J.; Honkala, K.; Häkkinen, H. The Redox Chemistry of Gold with High-Valence Doped Calcium Oxide. *Angew. Chem.* **2013**, *125*, 1464−1467.
(25) Lin, X.; Nilius, N.; Sterrer, M.; Koskinen, P.; Häkkinen, H.; Freund, H.-J. Characterizing Low-Coordinated Atoms at the Periphery of MgO-Supported Au Islands. *Phys. Rev. B* **2010**, *81*, No. 153406.
(26) Frondelius, P.; Häkkinen, H.; Honkala, H. Formation of Gold(I) Edge Oxide at Flat Gold Nanoclusters on an Ultrathin MgO Film. *Angew. Chem.* **2010**, *122*, 8085−8088.
(27) Benia, H.-M.; Myrach, P.; Gonchar, A.; Risse, T.; Nilius, N.; Freund, H.-J. Electron Trapping in Misfit Dislocations of MgO Thin Films. *Phys. Rev. B* **2010**, *81*, No. 241415(R).
(28) Prada, S.; Giordano, L.; Pacchioni, G. Nb-Doped CaO: An Efficient Electron Donor System. *J. Phys.: Condens. Matter* **2014**, *26*, No. 315004.
(29) Green, X.; Tang, W.; Neurock, M.; Yates, J. T. Insights into Catalytic Oxidation at the Dual Perimeter Sites. *Acc. Chem. Res.* **2014**, *47*, 805−815.
(30) Cui, Y.; Nilius, N.; Shao, X.; Baldofski, M.; Sauer, J.; Freund, H.-J. Adsorption, Activation and Dissociation of Oxygen on Doped Oxides. *Angew. Chem., Int. Ed.* **2013**, *52*, 11385−11387.
(31) Binnig, G.; Frank, K.; Fuchs, H.; Garcia, N.; Reihl, B.; Rohrer, H.; Salvan, F.; Williams, A. Tunneling Spectroscopy and Inverse Photoemission. *Phys. Rev. Lett.* **1985**, *55*, 991−994.
(32) Cui, Y.; Huang, K.; Nilius, N.; Freund, H.-J. Charge Competition with Oxygen Molecules Determines the Growth of Gold Particles on Doped CaO Films. *Faraday Discuss.* **2013**, *162*, 1−11.

DOI: 10.1021/acs.accounts.5b00018
Acc. Chem. Res. 2015, 48, 1532−1539